FRIDAY-AES-1121

Contributions of Microbial Community Metabolic Expression to Biogeochemical Cycling in a Highly Stratified Meromictic Pond over a Diel Cycle

Margrethe H. Serres[1], Petra Byl[2], Joe J. Vallino[3] Julie A. Huber[1]

[1]WHOI
(508)-289-3627
mserres@whoi.edu
[2]Univ of Hawai'i at Mānoa
[3]MBL

Abstract:

Earth's biogeochemical cycle result largely from a complex interaction of individual microscopic organisms through growth, competition and cooperation. Meromictic lakes represent unique ecosystems for investigating microbial biogeochemistry due to the steep chemical gradients that support distinct resident microbial communities that interact within and across these layers. Here, we investigated microbial communities and biogeochemistry in Siders Pond, a meromictic pond on Cape Cod, MA, by sampling 8 depths spanning aerobic to anaerobic habitats over a 24-hour diel cycle. Together with environmental characterization of the Siders Pond water column, we examined the gene content and transcription patterns of microbial communities and specific populations to understand the taxonomy and metabolism both through the water column and over time. Members of the Cyanobacteria, Proteobacteria, Actinobacteria, and Bacteroidetes dominated the upper layers of Siders pond while below the chemocline the Archaea, e.g. Woesearchaeota, were more abundant. The surface samples had the highest transcription levels followed by the samples collected at the transition between the oxic and anoxic conditions. Genes expressed in the upper layers were associated with oxygenic photosynthesis. High levels of phosphate and phosphonate transporter genes suggested phosphate limitation. Below the chemocline genes for anoxygenic photosynthesis, sulfate reduction, methanogenesis, and motility were among the highest expressed. Overall gene expression was highest during daylight. Changes in gene expression over time were detected for oxic and anoxic photosynthesis, carbon fixation, and motility. Other functions, e.g. sulfite reductase were expressed at high levels during the whole period. Expression trends and networks related to the 24 hour cycle will be presented and compared to a thermodynamic model developed for Siders that determines optimal metabolic pathway expressions based on the principle of maximum entropy production. Together, results facilitate our understanding of how microbial communities organize and coordinate microbial biogeochemistry in aquatic ecosystems.

Methods

Siders Pond was sampled over a 24 hour period by collecting water from eight depths over 7 casts (Fig 1B). Chemistry and microbial cell density were measured (Figs 1C, 1D). DNA and RNA were collected on 0.22 um Sterivex filters and immediately frozen. DNA was extracted with phenol chloroform while RNA was extracted, purified, and converted to cDNA. Metagenomic and metatransciptomic libraries were prepared and sequenced on an Illumina MiSeq. Paired-end reads were quality filtered, assembled, and annotated at JGI. Ribosomal RNA was removed from the metatranscriptome.

EMIRGE was used to reconstruct full length 16S rRNA genes from the metagenomes and the genes classified with Mothur. Relative abundances of the 16S rRNA genes were determined from the NormPrior EMIRGE output. The metagenomes were merged and the metatransciptome was mapped against the meta genome CDSs using Kallisto. Genes were grouped by their KEGG Orthology (KO) assignments and the transcripts per millions (TPMs) recalculated and normalized using means clustering, edgeR and the TMM method. Genes with the highest counts were extracted.

To compare the metatranscriptome profiles the vegan library in R was used to calculate a Jaccard dissimilarity index followed by an NMDS analysis with a binary distance (Fig. 3A). Clustering (Fig. 3B) of both genes (left) and samples (top) and samples associated with metabolism was done using Euclidean distance. Transcription of carbon, nitrogen, or sulfur metabolism were determined by summarizing the TPMs of the respective genes and calculating their percentage distribution with depth.

To search for genes showing periodicity in their expression patterns, a RAIN (Rhythmicity Analysis Incorporating Nonparametric methods) analysis was done for genes associated with metabolism. Genes with significant periodicity ($p<0.05$) were extracted and analyzed for the functions.

Conclusions

- The stratification of Siders Pond is reflected in the microbial community compositions and in the gene expression patterns.
- Distinct clusters suggests a depth-specific taxonomic and functional diversity. I.e. an abundance of Chlorobi and Sulfur and Nitrogen metabolism genes at 8m depth (Fig. 1A, Fig. 3C)
- Genes identified as having periodic signals may shed light on metabolisms that are linked to day-night cycling. Their pathways can help explain how microbial communities shift and reorganize over short temporal scales, as well as inform the modeling effort.

References

Miller, C.S. et al. 2011. EMIRGE: reconstruction of full-length ribosomal genes from microbial community short read sequencing data. doi.org/10.1186/gb-2011-12-5-r44.

Smid, M. et al. 2018. Gene length corrected trimmed mean of M-values (GeTMM) processing of RNA-seq data performs similarly in intersample analyses while improving intrasample comparisons. doi.org/10.1186/s12859-018-2246-7

Thaben, P.F. and P.O. Westermark. Detecting Rhythms in Time Series with RAIN. doi.org10.1177/0748730414553029

Vallino , J.J. and J.A. Huber. 2018. Using maximum entropy production to describe microbial biogeochemistry over time and space in a meromictic pond. doi.org/10.3389/fenvs.2018.00100

Acknowledgements

Thank you Leslie Murphy, Emily Reddington, and Suzanne Thomas for preparing sequence libraries and making chemistry measurements. Thank you Sarah Hu for help with data analysis and images.
Funding support : NSF-GEO 1451356.

Siders Pond

Fig. 1A

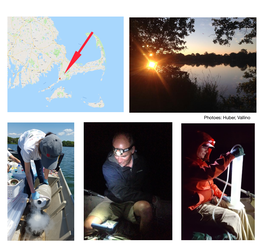

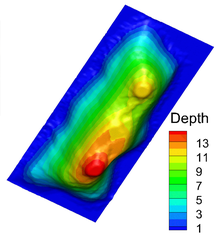

- Coastal pond in Falmouth, MA.
- Area: 14 hectares
- Maximum depth: 15m
- Meromictic; permanently stratified with no mixing of layers.
- Upper oxygenated layer, mixolimnion, is separated from lower anaerobic layer, monimolimnion, by a chemocline with increased salinity, phosphate, and nitrogen.

Fig. 1B

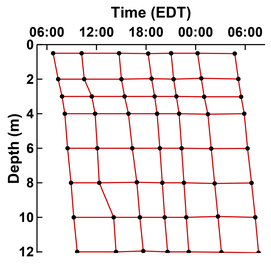

Fig. 1C

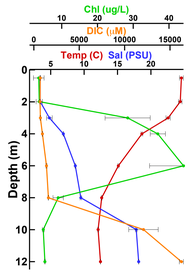

Fig. 1D

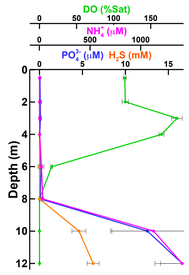

Abundance of microbes and gene transcripts.

Fig. 2A

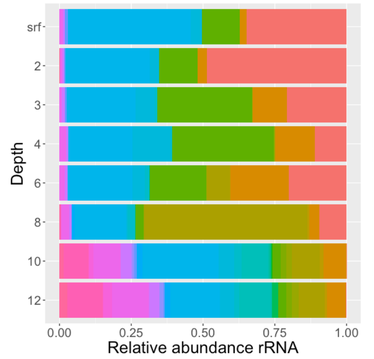

Table 2B

Depth	Gene Product	TPM
Surface	photosystem II P680 reaction center, PsbA	3010597
	arsenite transporter, ArsB	82217
	PTS system, ascorbate-specific IIB component	35909
	PTS system, phosphate-specific IIA componen, PstS	29768
	cytochrome c oxidase subunit 1, COX1	17204
	polyketide biosynthesis enoyl-CoA hydratase, PksI	16459
	acid phosphatase, class A, PhoN	14967
	photosystem II protein, PsbK	14524
	photosystem II cytochrome b559 subunit alpha, PsbE	10425
	F-type H+-transporting ATPase subunit alpha, AtpA	9577
3m	photosystem II P680 reaction center D1 protein, PsbA	140781
	arsenite transporter, ArsB	32989
	PTS system, phosphate-specific IIA componen, PstS	21051
	apocytochrome f, PetA	13383
	F-type H+-transporting ATPase subunit alpha, AtpA	13295
	PTS system, ascorbate-specific IIB component	12356
	polyketide biosynthesis enoyl-CoA hydratase, PksI	9831
	cytochrome c oxidase subunit 1, COX1	9328
	photosystem II protein, PsbK	7964
	photosystem I P700 chlorophyll a apoprotein A2, PsaB	6311
6m	photosystem II protein, PsbK	209498
	arsenite transporter, ACR3, arsB	33687
	photosystem II P680 reaction center D1 protein, PsbA	26741
	photosystem II cytochrome b559 subunit alpha, PsbE	22736
	polyketide biosynthesis enoyl-CoA hydratase PksI	20340
	phycocyanin alpha chain, CpcA	10030
	photosystem I P700 chlorophyll a apoprotein A2, PsaB	7928
	phycocyanin beta chain, CpcB	7439
	PTS system, phosphate-specific IIA componen, PstS	7318
	F-type H+-transporting ATPase subunit c	6142
8m	arsenate/arsenite/antimonite transcriptional repressor, ArsR	10373
	branched-chain amino acid transporter, LivK	8549
	superoxide reductase, Dfx	7996
	photosystem II P680 reaction center D1 protein, PsbA	7512
	acetyl-CoA synthetase, Acs	7219
	polyketide biosynthesis enoyl-CoA hydratase, PksI	6062
	arsenite transporter, ArsB	5635
	adenylylsulfate reductase subunit B, AprB	5365
	electron transport complex protein, RnfA	5000
	2-oxoglutarate/2-oxoacid ferredoxin oxidoreductase subunit, OorB	4982
12m	ABC glucose/mannose transport system IIA component, GtsA	12005
	ABC peptide/nickel transport system IIA component	10685
	polyketide biosynthesis enoyl-CoA hydratase, PksI	7279
	type IV pilus assembly protein, PilA	5633
	ABC branched-chain amino acid transport system IIA component, LivK	5473
	ABC sugar transport system IIA component	4274
	heterodisulfide reductase subunit A2, HdrA2	2886
	thioredoxin 1, TrxA	2754
	flagellin, FliC	2443
	formate dehydrogenase major subunit , FdhF	2274

A. Taxonomy of full length 16S rRNA sequences show distinct communities according to depth. Between 96 (surface) and 216 (10m) ribosomal sequences were reconstructed from each of the metagenomes. Three major community structures were detected corresponding to the mixolimnion (Proteobacteria, Actinobacteria, Cyanobacteria), chemocline (Chlorobi) and monimolimnion (Archaea, Omnitrophica, Proteobacteria, Plancomycetes) of Siders.

B. The most abundant gene transcripts from the Siders metatranscriptomes is listed according to the sample depths. Photosynthesis associated genes were most abundant in the three top layers while nutrient transport and genes associated with sulfur metabolism and methanogenesis were most abundant in the anaerobic layers. Arsenite detoxification genes were abundant in all layers except for the bottom.

Gene Expression over time and space

Fig. 3A

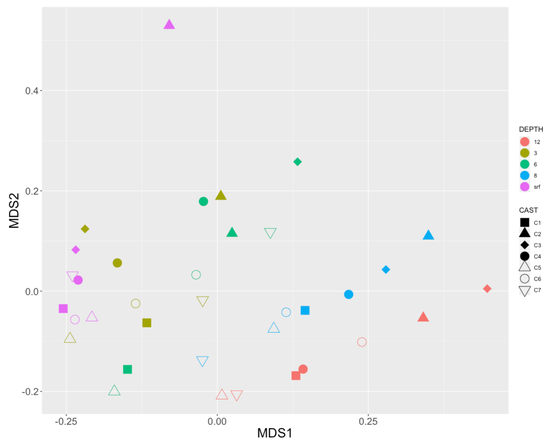

Fig. 3B

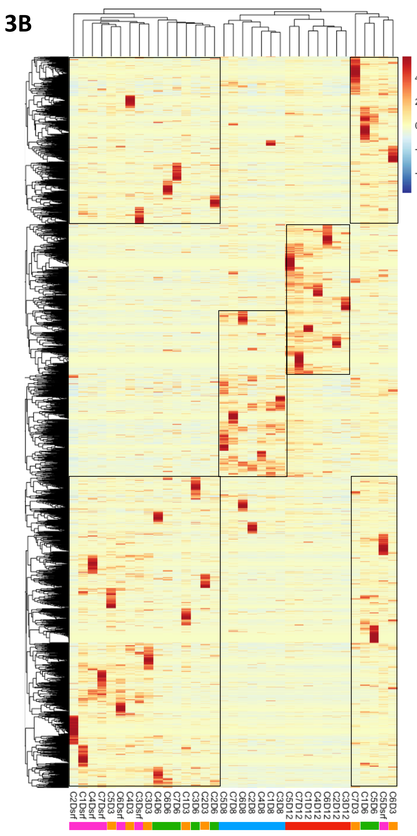

A. Siders Pond metatranscriptomes differ by depth and time of day. An NMDS analysis of all expressed genes (10147 KOs) showed four distinct clusters. The clusters were primarily separated by depth, clearly shown for 8 and 12m samples. A secondary separation by time of day (cast) was detected for the surface, 3m and 6M casts. (Stress 0.08)

B. Metabolic profiles at the KO level cluster by depth and time of day. Gene transcripts belong to the metabolism category (KEGG Orthology A09100, 5097 KOs). Colors represent high (red) to low (blue) using a Z-score transformation. Distinct clusters of genes were seen for samples collected at 8m and 12m. The genes expressed at the surface, 3m, and 6m clustered together. The latter depths constitute the mixolimnion where greater mixing is expected.

Fig. 3C

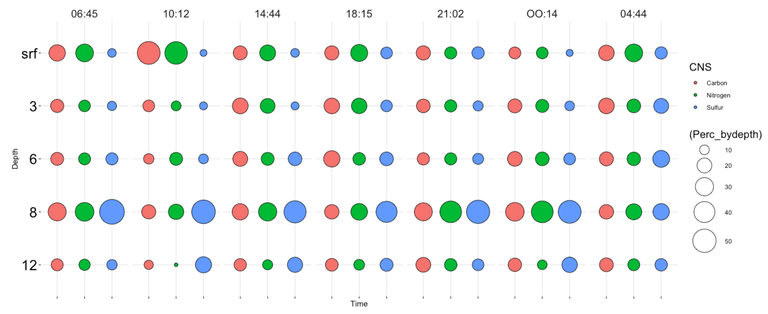

C. Expression of genes for Carbon, Nitrogen, and Sulfur metabolism vary according to sample depth. 1553 genes were included in the analysis. Sulfur metabolisms expressed at 8m included thiosulfate and sulfide oxidation, sulfur and sulfite reduction. Nitrogen metabolisms expressed at 8m include nitrate and nitrite reduction, nitrogen fixation and nitrification.

Periodicity

Table 4A

Metabolism	Dsrf	D3	D6	D8	D12
Carbon fixation	0	2	3	4	4
Carbon metabolism	8	10	3	8	7
Cell process	1	1	0	3	3
Cofactor metabolism	0	1	1	1	2
Energy metabolism	12	16	1	13	14
Hydrogen redox	1	0	0	0	2
Ion metabolism	1	0	0	1	2
Methane metabolism	1	0	1	2	2
Motility	2	0	0	2	2
Nitrogen metabolism	0	2	2	1	0
Sulfur metabolism	1	2	1	4	1
Transport	1	3	0	1	3
Genes with Significant Periodicity	28	37	12	40	42
Genes evaluated	405	409	481	616	491

Periodicity was detected for genes expressed at all depths. Periodicity was observed mainly for genes of energy and carbon metabolism. Only 3 genes were expressed with periodicity at both upper (surface, 3m, 6m) and bottom (8m and 12m) layers. Two genes showed periodicity in more than one upper layer and six genes in both bottom layers.

Modeling

Fig. 4A

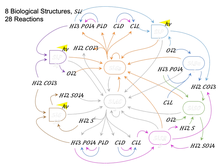

A Maximum Entropy Production based thermodynamic model developed for Siders Pond is used to predict optimal pathway usage for the system. The model consists of 28 reactions, and it is outlined in Fig.4A. Gene expression profiles over time and space extracted from the meta-transcriptome datasets are shown in Fig. 4B. Profiles of metabolic genes are compared to the expression levels predicted in themodel predictused to inform and refine the model (Fig. 4C).

Fig. 4B

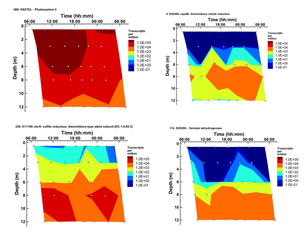

Fig. 4C